

Dalton Transactions

Accepted Manuscript



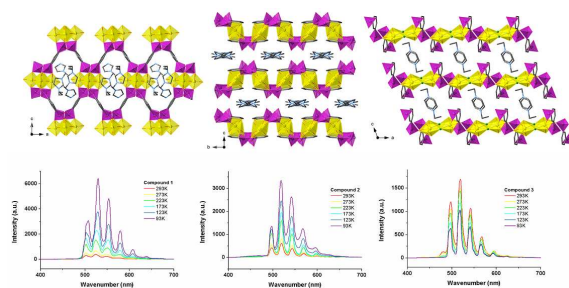
This is an *Accepted Manuscript*, which has been through the Royal Society of Chemistry peer review process and has been accepted for publication.

Accepted Manuscripts are published online shortly after acceptance, before technical editing, formatting and proof reading. Using this free service, authors can make their results available to the community, in citable form, before we publish the edited article. We will replace this *Accepted Manuscript* with the edited and formatted *Advance Article* as soon as it is available.

You can find more information about *Accepted Manuscripts* in the [Information for Authors](#).

Please note that technical editing may introduce minor changes to the text and/or graphics, which may alter content. The journal's standard [Terms & Conditions](#) and the [Ethical guidelines](#) still apply. In no event shall the Royal Society of Chemistry be held responsible for any errors or omissions in this *Accepted Manuscript* or any consequences arising from the use of any information it contains.

For Table of Content



Three new uranyl phosphonate compounds were synthesized *via* ionothermal method with one adopting chiral open framework consisting of achiral building units with protonated 1-methylimidazole cations filled in the channels, which are exchangeable for Cs⁺. These compounds were characterized by absorption, temperature dependent fluorescence, as well as infrared and Raman spectroscopies, establishing a structure-property relationship in this system.



Journal Name

ARTICLE

A New Chiral Uranyl Phosphonate Framework Consisting of Achiral Building Units Generated from Ionothermal Reaction: Structure and Spectroscopy Characterizations

Received 00th January 20xx,
Accepted 00th January 20xx

DOI: 10.1039/x0xx00000x

www.rsc.org/

Tao Zheng,^{a,b} Yang Gao,^{a,b} Lanhua Chen,^{a,b} Zhiyong Liu,^{a,b} Juan Diwu,^{*a,b} Zhifang Chai,^{a,b} Thomas E. Albrecht-Schmitt,^c Shuao Wang^{*a,b}

The ionothermal reactions of uranyl nitrate and 1,3-pbpH₄ (1,3-pbpH₄=1,3-phenylenebis(phosphonic acid) ligand in ionic liquids of [BMpyr]Br, [Epy]Br, and [Bmim][Dpb], respectively, afforded three new uranyl phosphonates, namely [C₄mim][[(UO₂)₂(1,3-pbpH)(1,3-pbpH)·Hmim] (1), [UO₂(1,3-pbpH₂H₂O·mpr] (2), and [Etpy][UO₂(1,3-pbpH₂F] (3). Compound 1 exhibits a rare example of a chiral uranyl phosphonate 3D framework structure built from achiral building units of tetragonal bipyramidal uranium polyhedra and 1,3-pbp ligands. The structure adopts a network with channels extending along the *b* axis, which are filled with C₄mim⁺ cations decomposed from BMpyr⁺ cations. In sharp contrast, compounds 2 & 3 both show pillared topology composed of uranyl pentagonal bipyramid polyhedra and phosphonate ligands. The layers are neutral in compound 2 with N-methylpyrrole molecules in the interlayer space, while compound 3 adopts anionic layer, and the charge is compensated with N-ethyl-pyridinium cations between the layers. Although compounds 1, 2, and 3 were synthesized under identical conditions with sole variation of the ionic liquid species, the resulting structures show a rich diversity in the local coordination environment of uranyl ions, the protonation of the phosphonate ligand, the conformation of ionic liquid ions, and the overall arrangement of the structure. All compounds were characterized by absorption, temperature dependent fluorescence, as well as infrared and Raman spectroscopies.

Introduction

Recently, several actinide based open framework structures have been reported, showing promising applications in nuclear waste separation and remediation processes. For instance, NDTB-1 is a thorium borate cationic network that could remove TcO₄⁻ from the simulated low level waste solution with high exchange capacity and selectivity.¹ The most recent example is a polycatenated uranyl carboxylate framework showing high resistance towards β and γ irradiation, as well as selective uptake ability of Cs⁺ ions from aqueous solutions.² The uranyl phosphonates are also promising materials in this field with nanotube³ or open framework structures that are able to exchange with ions as Cs⁺ or Co(en)₃^{3+,4}

On the other hand, chiral open framework materials are widely used in enantioselective separation, asymmetric catalysis etc. However, although chirality exists widely in the biological system, it is quite rare in the inorganic and inorganic/organic hybrid materials.⁵ R. E. Morris and X. Bu have summarized that the

synthetic approach towards chiral framework could be the utilization of chiral building blocks, chiral template, chiral solvent, and/or spontaneous crystallization from achiral units, while the last one is the least common and unpredictable route.⁵

Chiral uranyl phosphonates are exceedingly rare. A search in the CCDC database reveals that there are only four hydrothermally synthesized chiral uranyl phosphonate compounds reported, namely (UO₂)₃(bpH)₂(bp)₂·H₂O, [C₂H₁₀N₂][UO₂(C1P2)], [NEt₄][K[(UO₂)₃(C1P2)₂]]·1.5H₂O, and [NPr₄][UO₂(pmbH₃)(pmbH₂)H₂O]·2H₂O (bp = benzenephosphonic acid; C1P2 = methylenediphosphonic acid; pmb = *p*-xylenediphosphonic acid).^{4,6} The structure of [C₂H₁₀N₂][UO₂(C1P2)] and [NEt₄][K[(UO₂)₃(C1P2)₂]]·1.5H₂O are porous 3D framework. The (UO₂)₃(bpH)₂(bp)₂·H₂O and [NPr₄][UO₂(pmbH₃)(pmbH₂)H₂O]·2H₂O possesses 1D tubular and chain structure, respectively. All these structures were constructed from achiral units.

Introduced by Morris et al, ionothermal synthesis has opened a new route for preparation of functional materials, owing to the numerous choice of cations and anions for ionic liquids (ILs), which could be either hydrophobic or hydrophilic. In search of the chiral compound syntheses, chirality induced ionothermal synthesis route has been demonstrated to be non-trivial.⁷ The ionothermal method has been just applied in the synthesis of uranyl phosphonate system reported by Parker et al⁸ and Zheng et al⁹ originated from their importance in the spent nuclear fuel reprocess, especially the recent utilization of ionic liquid for solvent

^aSchool for Radiological and Interdisciplinary Sciences (RAD-X), Soochow University, Jiangsu 215123, China.

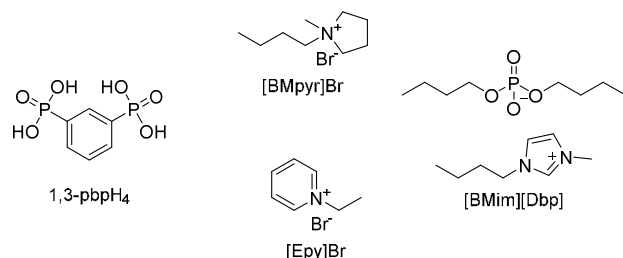
^bCollaborative Innovation Center of Radiation Medicine of Jiangsu Higher Education Institutions, Jiangsu 215123, China.

^cDepartment of Chemistry and Biochemistry, Florida State University, 95 Chieftain Way, Tallahassee, Florida 32306, United States.

† Electronic Supplementary Information (ESI) available: Synthesis of 1,3-phenylenebis(phosphonic acid), CD spectra, EDS and X-ray crystallographic files in cif format, for compound 1 - 3. See DOI: 10.1039/x0xx00000x

extraction process to replace organic solvent originated from its advantages such as low vapor pressure and nonflammability.

We report here a novel chiral uranyl phosphonate framework structure synthesized ionothermally as well as two other achiral layered compounds, namely $[C_4mim][[(UO_2)_2(1,3-pbpH)(1,3-pbpH)Hmim]]$ (**1**), $[UO_2(1,3-pbpH)_2H_2O\cdot mpr]$ (**2**), and $[Etpy][UO_2(1,3-pbpH)_2F]$ (**3**). (**1,3-pbpH**₄=1,3-phenylenebis(phosphonic acid); $[C_4mim][Dbp]$ =1-butyl-3-methylimidazolium dibutyl phosphate; $[C_4mpyr][Br]$ = N-butyl-N-methylpyrrolidinium bromide; $[Etpy][Br]$ =N-ethylpyridinium bromide; mpr = N-methylpyrrole; $Hmim$ = protonated 1-methylimidazole). The spectroscopic properties of those compounds were studied using room temperature UV-Vis absorption, temperature dependent fluorescence, IR and Raman spectroscopies. Compound **1** has shown preferred uptake of Cs^+ to Sr^{2+} from aqueous solutions. As an important message, here we have shown that the structures generated from ionothermal method deviates sharply from those of the traditional hydrothermal reaction for the uranyl system, which is similar to the observation reported in our previous work and by Parker et al.⁸⁻⁹



Scheme 1. Phosphonate ligands and ionic liquids used in this work.

Experimental Section

Caution! All studies and operations were conducted in an authorized laboratory to investigate actinide elements. Standard precautions should be performed for handling radioactive materials, as all uranium compounds used in these studies and operations contained depleted uranium.

Materials and Methods. 1,3-phenylenebis(phosphonic acid) (**1,3-pbpH**₄) was synthesized following a similar procedure reported in the literature¹⁰. The details of the synthesis is shown in the supporting information. $UO_2(NO_3)_2 \cdot 6H_2O$, solution of HF (40%), and ionic liquids were obtained from commercial sources (J&K Chemical, Sinopharm Chemical Reagent, and Lanzhou Greenchem ILs) and used as received.

Syntheses of Compound 1: A mixture of $UO_2(NO_3)_2 \cdot 6H_2O$ (0.05 mmol, 0.0256g), **1,3-pbpH**₄ (0.1 mmol, 0.0247 g), 1-butyl-3-methylimidazolium dibutyl phosphate (1 mmol, 0.3451g), and 1 drop of HF (40%), was placed in a 15 mL Teflon-lined stainless steel vessel and heated at 120 °C for 120 h, and then cooled to room temperature. IR (KBr, cm^{-1}): 3450(s,b), 3154(m), 3122(m), 3087(w), 2959(m), 2924(m), 2854(m), 1625(m), 1589(w), 1572(m), 1550(w), 1466(m), 1391(m), 1340(w), 1281(m), 1251(m), 1172(s), 1146(s), 1105(vs), 1075(vs), 1030(s), 982(vs), 909(s), 821(w), 800(m), 751(m), 698(m), 676(m), 630(w), 623(w), 574(s), 547(s), 531(s), 479(w), 439(m). Raman (cm^{-1}): 1585(m), 1539(w), 1459(w), 1414(w),

1385(w), 1342(w), 1179(w), 1091(w), 1015(m), 990(m), 820(s), 677(m), 411(m), 212(s), 175(m), 108(s), 83(s).

Syntheses of Compound 2: Yellow rhombic crystals of compound **2** were collected following the same process as compound **1**, except 1-butyl-3-methylimidazolium dibutyl phosphate was replaced by N-butyl-N-methylpyrrolidinium bromide (1 mmol, 0.2902g). IR (KBr, cm^{-1}): 3450(vs,b), 3164(w), 3063(w), 2991(w), 1625(m), 1592(m), 1473(w), 1403(m), 1255(s), 1209(s), 1189(s), 1169(vs), 1123(vs), 1102(s), 1078(s), 996(w), 942(m), 918(s), 837(s), 733(w), 699(m), 678(w), 650(w), 621(w), 552(s), 522(s), 502(s), 473(m), 442(w), 419(w). Raman (cm^{-1}): 1590(w), 1454(w), 1400(w), 1346(w), 1266(w), 1205(m), 1177(m), 1118(w), 1080(w), 1021(w), 992(m), 847(s), 679(m), 348(w), 273(m), 200(m), 135(s), 93(s).

Syntheses of Compound 3: Micro-crystals of compound **3** were obtained following the same process as compound **1**, except 1-butyl-3-methylimidazolium dibutyl phosphate was replaced by N-ethylpyridinium bromide (1 mmol, 0.1898g). IR (KBr, cm^{-1}): 3450(s,b), 3133(w), 3063(w), 2925(w), 2854(w), 1634(m), 1590(w), 1488(m), 1401(m), 1317(w), 1252(s), 1176(s), 1160(vs), 1120(vs), 1109(vs), 1097(s), 1080(vs), 1056(vs), 998(w), 984(w), 933(s), 908(vs), 824(m), 796(m), 784(m), 704(m), 685(m), 594(m), 577(m), 556(vs), 530(m), 512(m). 472(s), 461(m), 409(m). Raman (cm^{-1}): 1629(w), 1585(w), 1444(w), 1393(w), 1149(m), 1116(m), 1074(w), 1025(m), 986(m), 824(s), 761(w), 679(w), 645(w), 490(w), 411(w), 314(w), 261(m), 146(s), 83(s).

Crystallographic Studies. Single Crystals of compounds **1-3** were mounted on Cryoloops with paratone oil and optically aligned on a Bruker D8-Venture single crystal X-ray diffractometer equipped with a high-resolution digital camera. The diffraction data were collected using a CMOS detector at room temperature with a Turbo X-ray Source (Mo- $K\alpha$ radiation, $\lambda = 0.71073 \text{ \AA}$, 50kV/50mA power). The data was reduced by SAINT package of Bruker and the structures of all compounds were solved by the direct method and refined on F^2 by full-matrix least-squares methods using SHELXTL¹¹ (2014 version) and all the non-hydrogen atoms were refined anisotropically. The protons are difficult to locate since their electron densities are too low, thus all hydrogen atoms except those attached to water molecules were put in calculated positions. The hydrogen atoms of disordered IL cations were not added.

Absorption, Fluorescence, Infrared and Raman Spectroscopy. UV-Vis absorption spectroscopy were measured from single crystals of the compounds from 200 to 800 nm, using the Craic Technologies microspectrophotometer. Under the 365 nm irradiation, fluorescence spectra was recorded from 400 nm to 700 nm at 293, 273, 223, 173, 123, and 93 K, respectively. The room temperature infrared spectra were measured ($4000-400 \text{ cm}^{-1}$) on a Bruker VERTX 70 FT-IR instrument in transmittance mode. Raman spectra were collected in the range of $50-2000 \text{ cm}^{-1}$ with crystals placed on quartz slides without oil. Circular dichroism spectroscopy (CD) was performed on Circular dichroism spectrometer Model 410 (Biomedical, Inc.).

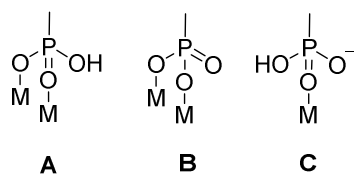
Results and Discussion

Structure Descriptions.

Table 1. Crystallography Data and Refinement Details for 1-3

	1	2	3
Formula	C ₂₄ H ₃₂ N ₄ O ₁₆ P ₄ U ₂	C ₁₇ H ₁₂ NO ₁₈ P ₄ U ₂	C ₁₃ H ₁₆ FNO ₈ P ₂ U
M	1232.48	1120.23	633.24
CCDC No.	1412606	1412603	1412604
Crystal system	Orthorhombic	Monoclinic	Triclinic
Space group	<i>P</i> 2 ₁ 2 ₁ 2 ₁	<i>I</i> 2/ <i>c</i>	<i>P</i> $\bar{1}$
<i>a</i> / Å	9.767(1)	17.691(1)	9.719(1)
<i>b</i> / Å	19.132(1)	9.241(1)	10.379(1)
<i>c</i> / Å	19.139(1)	19.823(1)	10.464(1)
α / °	90	90	110.067(2)
β / °	90	114.697(6)	103.971(2)
γ / °	90	90	105.105(2)
<i>V</i> / Å ³	3576.3(3)	2944.2(4)	891.3(1)
<i>Z</i>	4	4	2
ρ_{calcd} / g cm ⁻³	2.289	2.523	2.360
<i>F</i> (000)	2304	2044	592
\int (Mo-K α) / mm ⁻¹	9.298	11.283	9.337
Goof on <i>F</i> ²	1.052	1.032	1.203
<i>R</i> ₁ , <i>wR</i> ₂	0.0329,	0.0224,	0.0719,
[<i>I</i> > 2 σ (<i>I</i>)]	0.0551	0.0755	0.2064
<i>R</i> ₁ , <i>wR</i> ₂ (all data) ^a	0.0481,	0.0294,	0.0788,
	0.0587	0.1035	0.2090
($\Delta\rho$) _{max}	0.690,	1.594,	5.654,
($\Delta\rho$) _{min} / eÅ ⁻³	-0.931	-2.136	-7.156

$$^a R_1 = \sum ||F_o| - |F_c|| / \sum |F_o|, wR_2 = [\sum w(F_o^2 - F_c^2)^2 / \sum w(F_o^2)]^{1/2}$$



Scheme 2. Coordination modes of the phosphonate group.

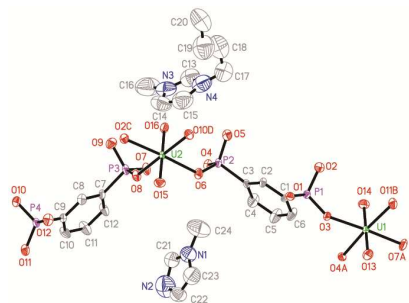
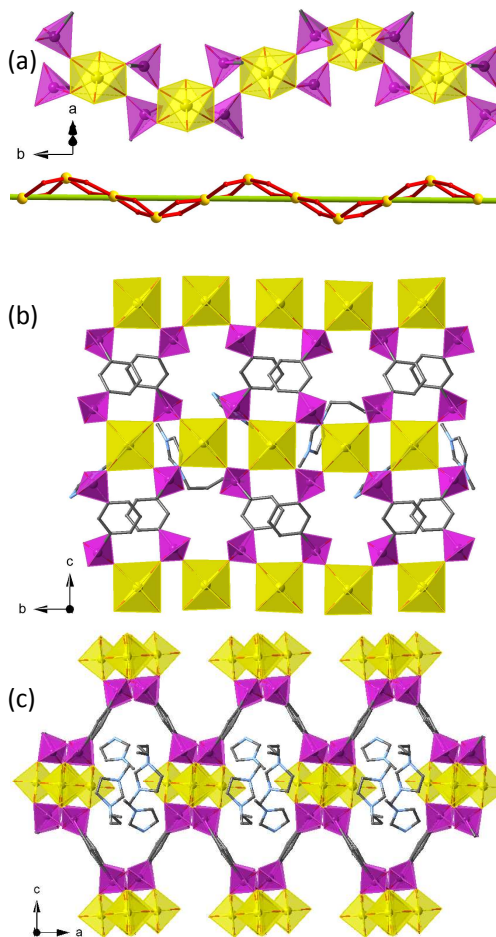


Fig. 1. Building unit of compound 1 with atomic labeling scheme at 50% probability, with all hydrogen omitted for clarity.

Fig. 2. A chiral chain of UO₇ units and CPO₃ tetrahedra along *b* axis (a) and the 3D structure was achieved by chiral chains further linked by organic moiety of 1,3-pbp ligand along *a* and *c* axis (b and c) of compound 1. UO₆ unit is represented by yellow tetragonal bipyramid, and CPO₃ is purple tetrahedron.Crystal structure of compound [C₄mim][(UO₂)₂(1,3-pbpH)(1,3-pbpH)·Hmim] (1)

Compound 1 crystallizes in a chiral orthorhombic space group *P*2₁2₁2₁ (Table 1). The structure was refined as an inversion twin, with a Flack parameter of 0.193(10), indicating that the crystal used for X-Ray diffraction was racemic conglomeration with one major enantiomer. This is consistent with the solid Circular Dichroism (CD) spectrum collected from a bulk sample of compound 1, whose signal is orientated from the excess of the major enantiomer (Fig. S3 in the supporting information). The asymmetric unit contains two UO₂²⁺ cations, two 1,3-pbp ligands, one protonated 1-methylimidazole cation and one 1-butyl-3-methylimidazolium cation, which are all located at general positions. As shown in Fig. 1, both UO₂²⁺ cation adopts tetragonal bipyramidal coordination geometry, forming UO₆ units. The CPO₃ moieties from the phosphonate ligands adopt two coordination modes of **A** and **B** with the uranyl centers graphed in Scheme 2. The four oxygen

atoms located in the equatorial plane are O3, O4A, O7A, and O11B for U1 and O6, O8, O2C, and O10D for U2, respectively, which are from four different 1,3-pbp ligands (symmetric codes for **3**: A: $x+1/2, -y+3/2, -z$; B: $x, y, z-1$; C: $-x+3/2, -y+2, z+1/2$; D: $-x+3/2, -y+2, z-1/2$). The U=O and U–O bond lengths are in the range of 1.767(6)–1.776(6) Å and 2.276(9)–2.297(9) Å, respectively (Table 2), which are in agreement with published bond lengths. Each 1,3-pbp ligand is coordinated to four uranyl centers since each CPO₃ moiety is bonded to two uranyl centers. In this manner, the UO₆ units are linked along *b* axis by the CPO₃ tetrahedron, yielding a chiral 1D uranyl phosphonate chain structure with 2₁ screw axis, and then further connected by phenyl rings of **1,3-pbp** ligands, resulting in a chiral 3D structure with two other 2₁ screw axis along *a* and *c* directions. The channels along the *b* axis are filled with C₄mim⁺ cations (Fig. 2). Hydrogen atoms were determined by analyzing the coordination environment of oxygen atoms and hydrogen bonds were found in O12–H5–O5 and O1–H9–O9, with the distance between oxygen and hydrogen atoms being 1.708 Å and 1.757 Å, respectively. It is noteworthy that such chiral structure built from achiral units are exceedingly rare in the uranyl compound, especially for framework structures, since the formation of such compound is arbitrary.⁴

Since the C₄mim⁺ cations filled in the voids are potentially capable to be replaced, an initial ion exchange experiment was conducted by soaking crystals of **1** in Cs⁺ and Sr²⁺ solutions. After this, the crystals were washed with distilled water and characterized with EDS (Energy Dispersive Spectroscopy) to determine the amount of Cs⁺ and Sr²⁺ sorbed by the crystals. The EDS results show that the uptake of Cs⁺ is higher than Sr²⁺, under similar conditions (Fig. S4 and S5), suggesting a decent exchange selectivity towards Cs⁺ possessed by compound **1**. The mechanism accounting for such an unexpected selectivity is under further investigation.

Table 2. Selected Bond Distances (Å) for compound **1**.

U1–O13	1.767(6)	P1–O1	1.516(9)
U1–O14	1.770(6)	P1–O2	1.52(1)
U1–O4A	2.276(9)	P1–O3	1.53(1)
U1–O7A	2.291(9)	P2–O5	1.509(9)
U1–O3	2.292(9)	P2–O4	1.51(1)
U1–O11B	2.297(9)	P2–O6	1.54(1)
U2–O16	1.771(6)	P3–O8	1.51(1)
U2–O15	1.776(6)	P3–O7	1.51(1)
U2–O2C	2.280(9)	P3–O9	1.54(1)
U2–O10D	2.285(9)	P4–O10	1.51(1)
U2–O8	2.291(9)	P4–O12	1.511(9)
U2–O6	2.290(9)	P4–O11	1.52(1)

Symmetric codes for **1**: A: $x+1/2, -y+3/2, -z$; B: $x, y, z-1$; C: $-x+3/2, -y+2, z+1/2$; D: $-x+3/2, -y+2, z-1/2$.

Crystal structure of compound [UO₂(1,3-pbpH₂)H₂O·mpr] (**2**)

Unlike compound **1**, compound **2** is a two-dimensional layered structure that crystallizes in monoclinic space group *C2/c* (Table 1), and the asymmetric unit contains one UO₂²⁺ cation, one 1,3-pbp ligand, one coordinated water molecule, and N-methylpyrrole with

half occupancy (Fig. 3). UO₂²⁺ cation adopts pentagonal bipyramid coordination geometry with five oxygen atoms located in the equatorial plane being from four CPO₃ moieties, and the fifth one is occupied by the water molecule (O1, O2A, O4C, O5B and O1w, symmetric codes for **2**: A: $-x+1/2, y-1/2, -z$; B: $x+1/2, -y+1/2, z$; C: $-x, -y, -z$). In contrast to **1**, the CPO₃ moieties from **1,3-pbp** ligand only coordinate to the uranyl centers with Mode **A** (Scheme 2). The layers can be best described as two layers of 1,3-pbp ligands that are linked to each other through the tilted uranyl monomers, together with the π - π stacking found in the structure for adjacent phenyl ring of **1,3-pbp** ligands, where the centroid-centroid distance between two phenyl rings is 3.591 Å (Fig. 4).¹²

The U=O and U–O bond lengths are in the range of 1.753(4)–1.758(4) Å and 2.358(3)–2.399(4) Å, respectively (Table 3), which agree with published bond lengths.^{3, 6a, 13} The bond distances of P1–O3 and P2–O6 are 1.551(4) and 1.557(3) Å, therefore O3 and O6 should be protonated. Those bond distances of the rest P and O in phosphonate groups are in the range of 1.476(4)–1.486(4) Å, [P1–O2, 1.485(4) Å; P1–O1, 1.486(4) Å; P2–O5, 1.476(4) Å; P2–O4, 1.486(4) Å], suggesting that those oxygen atoms are deprotonated. Thus, the layers of compound **2** was concluded to be neutral, with disordered N-methylpyrrole molecules filled in the interlayer space.

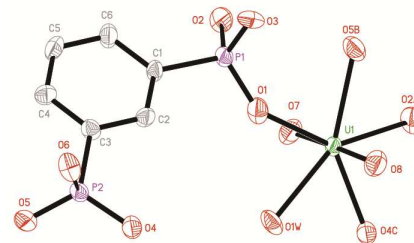
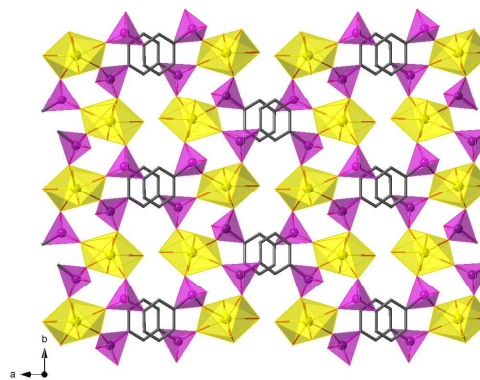


Fig. 3. Building unit of compound **2** with atomic labeling scheme at 50% probability, with all hydrogen atoms and N-methylpyrrole omitted for clarity.



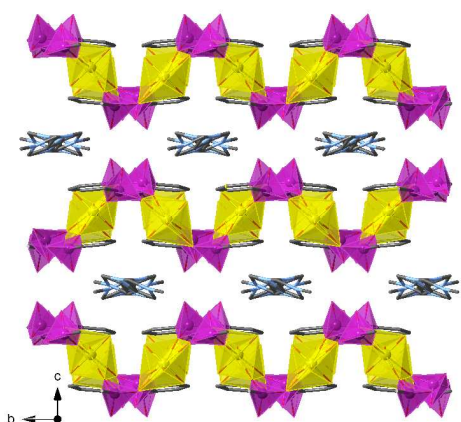


Fig. 4. 2D structure of compound **2** viewed along *c* and *b* axis (top) and (bottom). UO_7 is represented by yellow pentagonal bipyramid, CPO_3 is purple tetrahedron.

Table 3. Selected Bond Distances (Å) for compound **2**.

U1-O8	1.753(4)	P1-O2	1.485(4)
U1-O7	1.758(4)	P1-O1	1.486(4)
U1-O2A	2.358(3)	P1-O3	1.551(4)
U1-O5B	2.374(4)	P2-O5	1.476(4)
U1-O1W	2.378(4)	P2-O4	1.486(4)
U1-O4C	2.388(4)	P2-O6	1.551(3)
U1-O1	2.399(4)		

Symmetric codes for **1**: A: $-x+1/2, y-1/2, -z$; B: $x+1/2, -y+1/2, z$; C: $-x, -y, -z$.

Crystal structure of compound $[\text{Etpy}][\text{UO}_2(1,3\text{-pbpH}_2)\text{F}]$ (**3**)

Compound **3** crystallizes in triclinic space group $P\bar{1}$ (Table 1), and the asymmetric unit contains one UO_2^{2+} cation, one 1,3-pbp ligand, one fluorine atom, and one N-ethylpyridinium cation with half occupancy (Fig. 5). Similar with compound **2**, UO_2^{2+} cation adopts pentagonal bipyramid coordination geometry, forming a UO_7 unit, with five coordination sites located in the equatorial plane being O1, O2A, and O4C from three CPO_3 moieties and two fluorine atoms (symmetric codes for **3**: A: $-x+2, -y+1, -z$; B: $-x+1, -y+1, -z$; C: $x, y+1, z$). It is surprising that fluorine is incorporated into the structure, while first two compounds do not contain any fluorine atoms, indicated from the EDS measurements (supporting information). The uranyl polyhedra existed as a dimer by edge-sharing of two fluorine ions, which is further connected by the bridging 1,3-pbp ligand along *a* and *b* axis with bonding modes of both **A** and **C** (Scheme 2), yielding a negatively charged layered structure (Fig. 6). The N-ethyl-pyridinium cations were found filling between the layers through hydrogen network to construct the 3D structure. The $\text{U}=\text{O}$ and $\text{U}-\text{O}$ bond lengths are in the range of 1.73(2)–1.80(1) Å and 2.32(1)–2.37(1) Å, respectively (Table 5). U1-F1 bond is 2.34(1) Å, which is in the normal range of 2.289(4)–2.394 (1) Å.¹⁴ The bond distance of P1-O3 is 1.56(1) Å and P2-O6 is 1.55(2) Å, suggesting the protonation of O3 and O6.

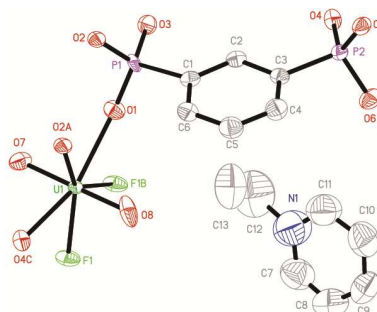


Fig. 5. Building unit of compound **3** with atomic labeling scheme at 50% probability, with all hydrogen omitted for clarity.

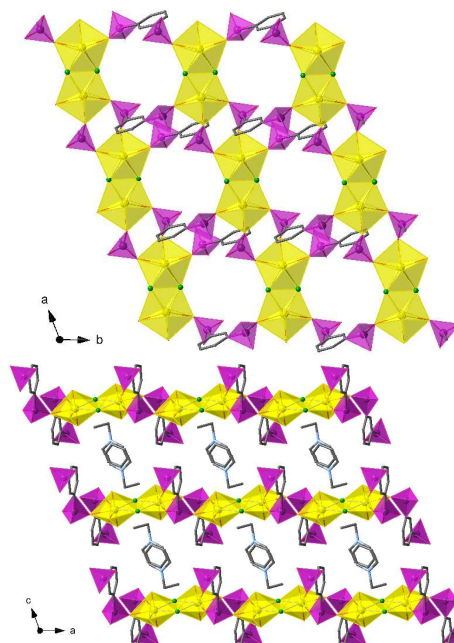


Fig. 6. 2D structure of compound **3** viewed along *c* (top) and *b* (bottom) axis. UO_7 is represented by yellow pentagonal bipyramid, CPO_3 is purple tetrahedron, and fluorine atom is green ball.

Table 4. Selected Bond Distances (Å) for compound **3**.

U1-O8	1.73(2)	P1-O2	1.53(1)
U1-O7	1.80(1)	P1-O1	1.53(1)
U1-O2A	2.32(1)	P1-O3	1.56(1)
U1-F1B	2.34(1)	P2-O4	1.52(2)
U1-F1	2.34(1)	P2-O5	1.52(1)
U1-O1	2.35(1)	P2-O6	1.55(2)
U1-O4C	2.37(1)		

Symmetric codes for **2**: A: $-x+2, -y+1, -z$; B: $-x+1, -y+1, -z$; C: $x, y+1, z$.

The Structural Deviation among Compounds **1**, **2**, and **3**:

We have previously reported the structural control of uranyl phosphonates under hydrothermal conditions via the alternation of pH, organic templates, and temperatures by analyzing the

coordination modes of uranyl to phosphonate ligands.^{6a} The results provide insight of how the protonation of phosphonate would affect the bonding between uranyl centers and phosphonate ligands, and correspondingly the overall structure dimensions. However in ionothermal synthesis, losing pH as a parameter of reaction conditions, Parker et al. proposed that the roles that the ligand, the flux method, as well as the ionic liquid conformation played were of equally importance in determining the crystal structure topology. Our previous work of uranyl pmb (p-xylenediphosphonic acid) compounds also demonstrated a large structural variation between compounds obtained hydrothermally and ionothermally, as they all show layered structure with cations of ionic liquid filled between the layers of uranyl phosphonates.⁹

Here in this work, compounds **1** to **3** were synthesized by using the same 1,3-bpp ligands under ionothermal conditions and solely varying the ionic liquid species. Besides the most significant variation among the three compounds, where **1** is an extremely rare sample of chiral uranyl phosphonate framework with exchangeable cations from the ionic liquid, while **2** and **3** are both pillared structures, detailed structural comparison reveals that these structures differ in uranyl local coordination environment, protonation of the phosphonates, structure dimension, and the ionic liquid configuration as listed in Table 6. From the view of the local environment of the uranyl unit, in compound **1**, it is connected to four oxygen atoms from four CPO₃ moieties, while four oxygen atoms and one water molecule are connected to the uranyl unit in **2**, and three oxygen atoms and two fluorine atoms in **3**. The water molecules are probably from the uranyl nitrate hexahydrate starting materials, whereas fluorine atoms are from the HF used in the reaction as mineralizing agent. The coordination mode analysis of the CPO₃ moiety shows that in both **A** and **C** mode, the phosphonate ligands are protonated, whereas in **B** mode, they are fully deprotonated. In mode **A**, two uranyl atoms (in compound **1**, and **2**) or uranyl dimers (in compound **3**) are bridged to give uranyl phosphonate chains. Modes **C** was adopted for connecting uranyl with phosphonates to get layer structures. The combination of mode **A** and **B** upgrades the overall structural dimensionality observed in **1**. This is consistent with our previous study, which shows that by controlling the magnitude of protonation of the ligand, it is possible to obtain target compound with expected dimensionality.

Table 5. Reaction Condition and Structure Comparison of Compounds **1-3**.

Comp.	Mode	ILs	D	G	C
1	A, B	[C ₄ mim][Dbp]	3D	UO ₆	[C ₄ mim]&[mim]
2	A	[C ₄ mpyr]Br	2D	UO ₇	[mpr]
3	A, C	[Etpy]Br	2D	UO ₅ F ₂	[Etpy]

G: Coordination geometry of U(VI); C: Cations or Molecules filled in the frameworks.

It is also quite interesting to find in compound **1** that the cation of the ionic liquid undergoes an in situ decomposition from 1-butyl-3-methylimidazolium to 1-methylimidazole, providing an alternate preparation of a desired cation initiated with a more complex starting material.

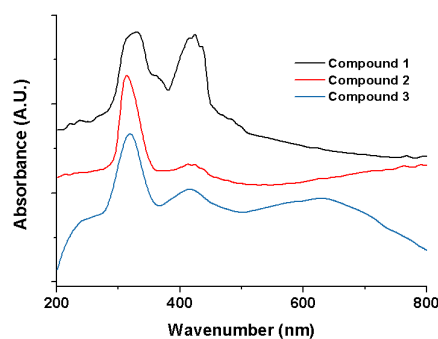


Fig. 7. UV-Vis spectra of compounds **1-3**. The spectra are elevated for clarity.

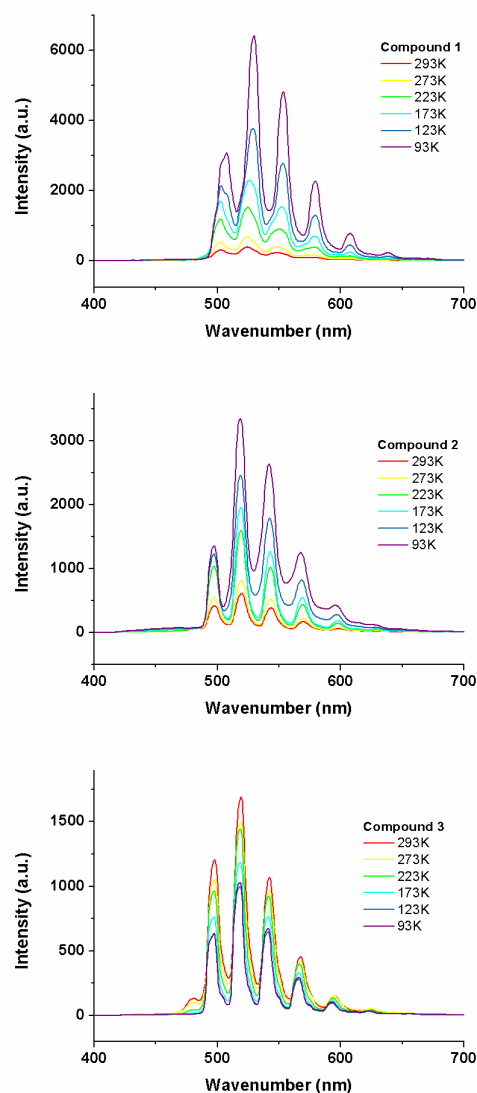


Fig. 8. Fluorescence spectra at different temperature of compound **1-3**.

Spectroscopic Properties.

The UV-Vis absorption spectra of three compounds shown in Fig. 7 all adopt two major peaks. The peaks near 320 nm (313.6 for **1**, 319.1 for **2**, and 330.1 for **3**) are resulted from the ligand to metal charge transfer of the uranyl unit, owing to the hybridization of the uranium 5f orbitals and the oxygen 2p orbitals, while the peaks around 420 nm are originated from the vibronically coupled charge transfer within the uranyl unit.¹⁵ The relative intensity between the two peaks were similar of compound **2** and **3**, while the 420 nm peak is much stronger in compound **1**, probably owing to the higher symmetry of the uranyl centers.

Table 6. Peaks of Fluorescence Spectra For compound 1-3

compounds	Peaks
1	508(m), 529(vs), 553(s), 579(m), 607(w), 639(vw)
2	498(m), 519 (vs), 542(s), 568(m), 595(w), 625(vw)
3	498(m), 519(vs), 542(s), 568(m), 595(w), 624 (vw)

The fluorescence spectra of the three compounds were collected from 200 nm to 800 nm at temperatures of 293, 273, 223, 173, 123, and 93K, respectively. The observed charge-transfer based emissions of yellow-green light in the range of 500-600 nm are mainly ascribed to the LUMO-HOMO electronic transitions coupled with symmetric and antisymmetric stretch vibrations of the nearly linear O≡U=O unit^{14f, 15} as shown in Fig. 8, which are typical in uranyl compounds.^{14a, 14c, 16} Notably, the intensities of fluorescence spectra of compounds **1** and **3** increase with the decrease of temperature, while the trend for compound **2** is reversed, likely due to the effect of fluorine coordination which provides a different thermal quenching process. For those uranyl units with tetragonal bipyramid coordination geometry, they commonly present weaker luminescence signals than the pentagonal or hexagonal bipyramidal geometry ones, attributed to the strict central symmetry of the uranyl site. However, the luminescence signal for uranyl units in compound **1** with tetragonal bipyramid coordination geometry is quite strong, which is likely due to the breakdown of strict central symmetry of uranyl units induced by overall chirality of the structure.

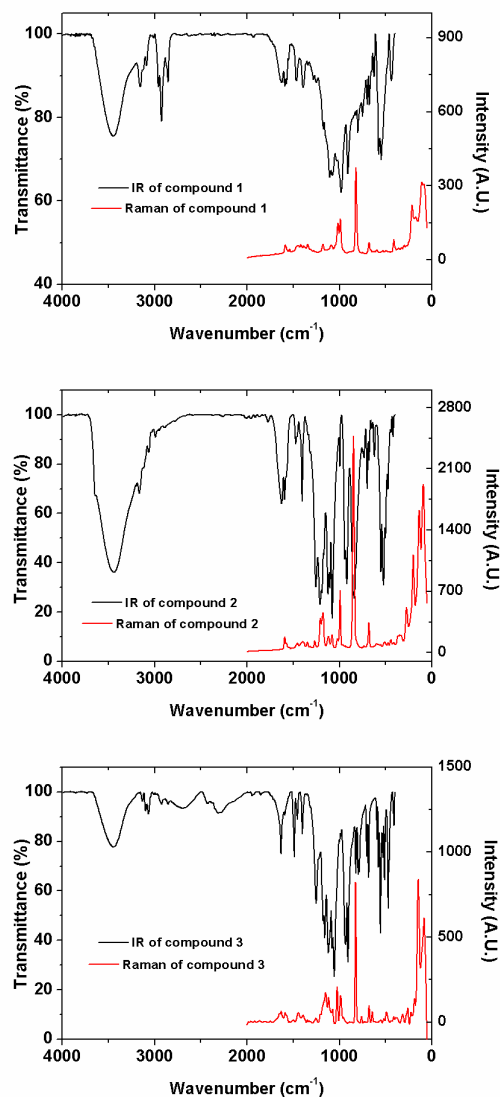


Fig. 9. IR and Raman spectra of compounds 1 - 3.

Infrared (IR) and Raman spectra were also recorded for all three compounds (Fig. 9). For IR spectra, the peaks between 3800 and 2500 cm^{-1} are mainly assigned to the stretch of O-H from phosphonates and C-H from organic moieties. The peaks appearing in the range of 1640 - 1390 cm^{-1} are assigned to the stretch of benzene ring or cations from ILs. The typical anti-symmetric and symmetric stretch peaks of P=O and P-O in the range of 1250 to 950 cm^{-1} are observed in these compounds.¹⁷ The anti-symmetric and symmetric stretch peaks of O≡U=O are active in IR and Raman, respectively, and therefore are assigned (918 and 847 cm^{-1} for **2**, 908 and 824 cm^{-1} for **3**, and 909 and 820 cm^{-1} for **1**).

Conclusions

In summary, three new uranyl phosphonate compounds have been obtained successfully by using phosphonate ligand and ionic liquids as both the solvent and structural template agents. Among

them, compound **1** shows a three dimensional chiral framework structure that is capable to uptake extraordinarily high amount of Cs⁺ ion with much better selectivity over Sr²⁺. The other two adopt common layered topologies for uranyl compounds. A detailed structural comparison reveals that the protonation of the phosphonate ligand would affect the coordination modes between uranyl unit and CPO₃ moieties, which therefore determines the overall dimension of the structure. The absorption and fluorescence spectra of the three compounds show deviation to some extent, which is most probably originated from different ligand donors.

Owing to the numerous choice of cation and anion combinations for the ionic liquids, ionothermal synthesis provides extremely high opportunity toward the findings of new structures. However, the rational designed synthesis would heavily depend on a thorough understanding of the current ionothermal products. By varying only one parameter at one time, it will be better and easier to elucidate the role it played during the reaction. Thus, our future work will first focus on the cation portion of the ionic liquid to study how it will affect the protonation of the ligand, aiming at better control of the overall structure.

Acknowledgements

We are grateful for funding supported by National Science Foundation of China (91326112, 21422704, 21471107, 81402628), the Science Foundation of Jiangsu Province (BK20140007, BK20140303), a Project Funded by the Priority Academic Program Development of Jiangsu Higher Education Institutions (PAPD), and "Young Thousand Talented Program" in China. Support for TEA-S was provided by the Chemical Sciences, Geosciences, and Biosciences Division, Office of Basic Energy Sciences, Office of Science, Heavy Elements Chemistry Program, U.S. Department of Energy, under Grant DE-FG02-13ER16414.

References

- (a) S. Wang, E. V. Alekseev, J. Diwu, W. H. Casey, B. L. Phillips, W. Depmeier and T. E. Albrecht-Schmitt, *Angew. Chem. Int. Ed.*, 2010, **49**, 1057; (b) S. Wang, P. Yu, B. A. Purse, M. J. Orta, J. Diwu, W. H. Casey, B. L. Phillips, E. V. Alekseev, W. Depmeier, D. T. Hobbs and T. E. Albrecht-Schmitt, *Adv. Funct. Mater.*, 2012, **22**, 2213.
- Y. Wang, Z. Liu, Y. Li, Z. Bai, W. Liu, Y. Wang, X. Xu, C. Xiao, D. Sheng, J. Diwu, J. Su, Z. Chai, T. E. Albrecht-Schmitt and S. Wang, *J. Am. Chem. Soc.*, 2015, **137**, 6144.
- P. O. Adelani and T. E. Albrecht-Schmitt, *Angew. Chem. Int. Ed.*, 2010, **49**, 8909.
- J. Diwu and T. E. Albrecht-Schmitt, *Chem. Commun.*, 2012, **48**, 3827.
- R. E. Morris and X. Bu, *Nat Chem*, 2010, **2**, 353.
- (a) T. Zheng, Q.-Y. Wu, Y. Gao, D. Gui, S. Qiu, L. Chen, D. Sheng, J. Diwu, W.-Q. Shi, Z. Chai, T. E. Albrecht-Schmitt and S. Wang, *Inorg. Chem.*, 2015, **54**, 3864; (b) D. M. Poojary, A. Cabeza, M. A. G. Aranda, S. Bruque and A. Clearfield, *Inorg. Chem.*, 1996, **35**, 1468.
- Z. Lin, A. M. Z. Slawin and R. E. Morris, *J. Am. Chem. Soc.*, 2007, **129**, 4880.
- T. G. Parker, J. N. Cross, M. J. Polinski, J. Lin and T. E. Albrecht-Schmitt, *Cryst. Growth Des.*, 2013, **14**, 228.
- T. Zheng, Y. Gao, L. Chen, J. Diwu, Z. Chai, T. E. Albrecht-Schmitt and S. Wang, *Inorg. Chim. Acta*, 2015, **435**, 131.
- S. S. Iremonger, J. Liang, R. Vaidhyanathan and G. K. H. Shimizu, *Chem. Commun.*, 2011, **47**, 4430.
- G. M. Sheldrick, *SHELXTL, Siemens Analytical X-ray Instruments, Inc: Madison, WI, 2001*.
- (a) C. Janiak, *J. Chem. Soc., Dalton Trans.*, 2000, 3885; (b) C. A. Hunter and J. K. M. Sanders, *J. Am. Chem. Soc.*, 1990, **112**, 5525.
- (a) S.-S. Bao, G.-S. Chen, Y. Wang, Y.-Z. Li, L.-M. Zheng and Q.-H. Luo, *Inorg. Chem.*, 2006, **45**, 1124; (b) H. Y. Wu, W. T. Yang and Z. M. Sun, *Cryst. Growth Des.*, 2012, **12**, 4669; (c) K. E. Knope and C. L. Cahill, *Inorg. Chem. Commun.*, 2010, **13**, 1040.
- (a) P. O. Adelani, A. G. Oliver and T. E. Albrecht-Schmitt, *Cryst. Growth Des.*, 2011, **11**, 3072; (b) A.-G. D. Nelson, E. V. Alekseev, R. C. Ewing and T. E. Albrecht-Schmitt, *J. Solid State Chem.*, 2012, **192**, 153; (c) P. O. Adelani, A. G. Oliver and T. E. Albrecht-Schmitt, *Cryst. Growth Des.*, 2011, **11**, 1966; (d) P. O. Adelani and T. E. Albrecht-Schmitt, *Inorg. Chem.*, 2011, **50**, 12184; (e) P. O. Adelani and T. E. Albrecht-Schmitt, *J. Solid State Chem.*, 2011, **184**, 2368; (f) P. O. Adelani and T. E. Albrecht-Schmitt, *Cryst. Growth Des.*, 2011, **11**, 4227.
- (a) J. Su, K. Zhang, W. H. E. Schwarz and J. Li, *Inorg. Chem.*, 2011, **50**, 2082; (b) P. O. Adelani and T. E. Albrecht-Schmitt, *Cryst. Growth Des.*, 2012, **12**, 5800; (c) P. O. Adelani and T. E. Albrecht-Schmitt, *J. Solid State Chem.*, 2012, **192**, 377.
- Q. Zhu, R. Shang, S. Chen, C. Liu, Z. Wang and S. Gao, *Inorg. Chem.*, 2014, **53**, 8708.
- D. Grohol and A. Clearfield, *J. Am. Chem. Soc.*, 1997, **119**, 4662.